DECIPHERING THE EFFECT OF NEMALIN-MYOPATHY NEBULIN MUTATIONS ON DESMIN BINDING

A Senior Scholars Thesis

by

KRYSTYNA MARIE JACOBS

Submitted to the Office of Undergraduate Research
Texas A&M University
in partial fulfillment of the requirements for the designation as

UNDERGRADUATE RESEARCH SCHOLAR

April 2010

Major: Biomedical Science

DECIPHERING THE EFFECT OF NEMALIN-MYOPATHY NEBULIN MUTATIONS ON DESMIN BINDING

A Senior Scholars Thesis

by

KRYSTYNA MARIE JACOBS

Submitted to the Office of Undergraduate Research
Texas A&M University
in partial fulfillment of the requirements for the designation as

UNDERGRADUATE RESEARCH SCHOLAR

Approved by:

Research Advisor: Gloria M. Conover
Associate Dean for Undergraduate Research: Robert C. Webb

April 2010

Major: Biomedical Science

ABSTRACT

Deciphering the Effect of Nemaline-Myopathy Nebulin Mutations on Desmin Binding.
(April 2010)

Krystyna Marie Jacobs
Department of Biomedical Science
Texas A&M University

Research Advisor: Dr. Gloria M. Conover
Department of Veterinary Pathobiology

Our research focuses on the role of intermediate proteins in human disease. Desmin, a major intermediate filament protein in muscle cells, is organized into a central coiled-coil alpha helical domain flanked by globular head and tail domains. Our goal is to decipher the functional significance of the association of desmin to the giant thin filament protein nebulin at the sarcomeric Z-discs and its relation to muscle disease. Mutations in nebulin cause nemaline myopathy, a debilitating genetic muscle disease that affects children and adults alike. Previous research has shown that nebulin has a high affinity binding to desmin. However, little is known about the contribution of lower affinity binding desmin domains to nebulin or about the involvement of this interaction in nemaline myopathy. We hypothesize that the desmin 3-dimensional linkage to nebulin contributes to nemaline myopathy pathology. To test our hypothesis, we tested the binding profile of a nebulin-associated nemaline myopathy mutation to particular desmin domains using biochemical approaches. Our ELISA and GST-pull down assays showed that nebulin modules 160-164 bind to desmin's central rod coil 2b

and tail subdomains. Moreover, we found significantly decreased binding of the desmin coil 2b to the nemaline myopathy Nebulin M160-164 T5681P mutant as compared to nebulin M160-164. A 3-fold binding increase of the coil 2b was found in random alanine nebulin M160-164 L5646A mutant as compared to nebulin nemaline-associated nebulin M160-164 T5681P mutant, underscoring the importance of this region to the interaction of desmin and nebulin. Taken together, our findings suggest that differences in the binding profile of nemaline-associated nebulin mutations to desmin may contribute to our understanding the underlying molecular mechanism responsible for this disease. This knowledge may be significant because it may aid in devising new treatments for nemaline myopathy patients in the future.

ACKNOWLEDGMENTS

I would like to thank Dr. Gloria M. Conover in the Department of Veterinary Pathobiology at the College of Veterinary Medicine and Biomedical Sciences at Texas A&M University for her support as my sponsor for this research project in her laboratory, for sharing her knowledge with me and for her continued effort to help me succeed. Thanks to Andrew Coronado, Samaneh Karami and to Kristen Timberlake for their help on various experiments that I could not finish alone. I would like to give a special thanks to Samaneh for allowing me to use her data for figure 10 and in the 13th Undergraduate Research Week poster presented on March 25th, 2010. With her help the poster was awarded session winner and 1st place in the Microbiology category. This Thesis was funded by a Scientist Development Grant from the American Heart Association and Texas A&M start-up funding to Gloria Conover.

NOMENCLATURE

NM	Nemaline myopathy
IF	Intermediate filaments
WT	Wild-type protein
Min	Minutes
H	Hours
RT	Room temperature (25ºC)
ON	Overnight incubation

TABLE OF CONTENTS

Page

CHAPTER Page

LIST OF FIGURES

CHAPTER I

INTRODUCTION

The cytoskeleton of a cell is composed of fibrillar three major cytoplasmic elements. These fibrillar elements are intermediate filaments (IFs), microfilaments (MFs), and microtubules (MTs). Our research focus is on the main intermediate filament muscle protein, desmin, its linkage to the contractile apparatus, and its contribution to muscle disease. IF proteins are grouped into six types (I-VI); types I-IV are found in the cytoplasm, type V is found in the nucleus and type VI is found in the lens of the eye. Desmin is a type III IF protein and mutations in desmin are known to cause debilitating cardiomyopathies and skeletal myopathies. (Omary, 2009). IFs are important for cell function because they create the backbone of the cell acting as major mechanosensors and mechanotransducers for various cell processes including cell migration, respiration and organelle trafficking (Reviewed in Herrmann *et al.*, 2007).

Remarkably, in the last 20 years, over 80 human diseases have been associated with mutations in IFs. For example, keratin 14 was the first IF to be associated with a human disease called Epidermolysis bullosa simplex. From this discovery, scientists realized that there are a large amount of Mendelian-inherited diseases caused by mutations in genes that encode IF-proteins (Omary, 2009).

This thesis follows the style of Molecular Biology of the Cell.

Our research focuses on the contribution of the desmin linkage to the contractile apparatus and how this may relate to disease states such as nemaline myopathy (NM). Nemaline myopathy is caused by inherited mutations in muscle proteins; nebulin, tropomyosin, actin, troponin and cofilin (Reviewed in Sanoudou and Beggs, 2001). It is a non-progressive disease of the voluntary muscles, caused in most cases by mutations in the actin-binding thin filament protein nebulin NEM 2. Clinical phenotypes are highly heterogeneous; and patients exhibit different ages of onset and severity. Though the clinical signs are variable, there are some that are common to all nemaline myopathies. These are moderate to severe weakness in leg, arm and trunk muscles; mild to moderate weakness of the face, tongue and throat muscles; the reflexes are decreased or absent; high-arched feet, curvature of the spine and jaw malformation may also be observed. The worse form of NM appears at birth, children will have marked weakness and lack of muscle tone, and death will occur in the first few years due to respiratory failure.

Anatomy of the sarcomere

There are two major systems that help the sarcomere contract and relax. These are the thin and thick filament systems; actin and myosin are the major proteins that constitute the framework of this minimal contractile unit. Myosin is a thick filament associated with the center of the sarcomere; its main function is to interact with actin and utilize energy from ATP hydrolysis to generate mechanical force (contractions). Actin is part of the thin filament system; it is intertwined with nebulin and acts as the scaffold on which myosin can generate force for contractions in the sarcomere. Desmin is an intermediate

filament that has a mix of alpha-helical and non-helical structures. These three elements, thin, thick and intermediate filaments, bind together to create the cytoskeleton that each contractile cell relies on to generate force. Mutations in any region of this network can cause mild to severe myopathies. Desmin and nebulin myopathies and the mutations that cause them are the focus of our research.

Desmin structure and muscle disease

Desmin was discovered in the early 1970's (Lazarides and Hubbard, 1976). It is expressed in cardiac, skeletal and smooth muscle. It connects with other proteins in the cell to create a continuous cytoskeletal network that maintains a spatial relationship with the contractile apparatus and other structural elements. This helps the cell to maintain its cellular integrity (Reviewed in Goldfarb and Dalakas, 2009). Desmin is organized into three domains; a highly conserved α-helical core of 308 amino acid residues that is flanked by globular N- and C- terminal regions. The N-and C- regions are known as the 'head' and 'tail' regions, respectively. The helical core has a seven residue (heptad) repeat pattern that guides two polypeptides to for a homopolymeric coiled-coil dimer. The heptad periodicity within the helical rod is interrupted in several places. This results in four helical segments known as 1A, 1B, 2A, and 2B; which are connected by nonhelical linkers (Reviewed in Goldfarb and Dalakas, 2009).

Desmin IFs form a tetramer that consists of homopolymers (Reviewed in Herrmann *et al.*, 2007). During assembly in the cytoplasm, desmin combines with other desmin

tetramers to form unit-length filaments (ULFs). These bind with other ULFs and short filaments to eventually form a radially compacted protein (Herrmann *et al.*, 2009). Desminopathy is characterized by mutations in the protein desmin, which in some cases has been demonstrated to interfere with the normal filament assembly by *in vitro* assembly assays and cardiac cells (Bar *et al.*, 2005a). 45 known disease-causing desmin mutations have been reported; 40 of the mutations are missense, 3 are small in-frame mutations, 1 is an exon-skipping mutations and 1 is an insertion that results in premature translation termination (Reviewed in Goldfarb and Dalakas, 2009). The disease is almost always characterized by increased amount of desmin within the sarcomere present as aggregates (Goebel, 1995). The clinical signs of desminopathy are skeletal muscle weakness associated with cardiac conduction blocks, arrhythmias, and restrictive heart failure.

Nebulin family structure and muscle disease

Nemaline myopathy (NM) is categorized as a form of congenital myopathy (Youssef *et al.*, 2009). Most of the NM cases are due to mutations in the large thin filament protein nebulin. Nebulin was discovered in the early 1980's (Wang, 1981). Each of the central modules (M1-180) directly interacts with actin monomers contained within the thin filaments of muscle (Panaviene *et al.*, 2007). Nebulin is a 600-900 kDa giant protein that is localized on the actin thin filament of striated muscle. The structure of nebulin is highly repetitive, due to the modules that are 30-35 amino acid residues long and arranged into simple and super repeats. Nebulin's central region contains 22 of these

super repeats; each has seven 35-residue simple repeats within them. The actin binding site is identified by the SDXXYK-motif, which is repeated. Nebulin has an 8-kDa N-terminal and a 20-kDa C-terminal; both have unique protein domains. Within the C-terminus there is a conserved src homology (SH3) domain; which may bind titin. α-actin anchors this terminus to the Z-disc of the muscle sarcomere. The Z-disk peripheral region binds desmin (Bang et al., 2002; Conover et al, 2009).

The N-terminus of nebulin binds tropomodulin at the pointed end of the thin filament (McElhinny *et al.*, 2001). Tropomodulin acts to bind and cap the pointed end of actin, and studies have shown that it plays a role in regulating the length of actin filaments in striated muscle. *In vivo* research has given evidence that nebulin functions in thin filament regulation, helps maintain physiological Z-disc length and assists in myofibrillar connectivity (Tonino *et al.*, 2010). Recent mouse knock-out studies have shown than nebulin stabilizes the thin filament rather than functions as a ruler for thin filament length (Ottenheijm *et al.*, 2009). Emergent nebulin isoforms are thought to function in a similar fashion as nebulin in skeletal muscle. The proteins are all modular proteins with the defining structure being the presence of the 35-residue nebulin modules. The isoforms are nebulette, N-RAP, LASP-1, and LIM-nebulette (Panaviene and Moncman, 2007).

Nebulin and nebulette: actin binding proteins

Nebulin was identified in 1981 as a major component of skeletal muscle (Wang, 1981). Nebulette, identified in 1995, is a cardiac nebulin- like protein has a mass of 107 kDa

(Moncman and Wang, 1995). It was demonstrated that nebulette is present in extracts of heart tissue from a variety of species; chickens, mice and rabbits, and that this protein is located in the I-Z-I complex of developing cardiomyocytes and isolated myofibrils (Moncman and Wang, 1995). Nebulette associates with the Z-lines of cardiac muscle sarcomeres.

Previously nebulin was thought to be a molecular ruler because it was found to extend the length of the thin filament (Kruger *et al.*, 1991). Its role at a molecular ruler would be to specify thin filament lengths during myofibrillar assembly. Once the thin filament reached the same length as nebulin, it directs Tmod capping to cut the end of the thin filament. Measured actin dynamics in skeletal and cardiac muscle do not follow the idea of nebulin as a molecular ruler. Thin filaments must be continually regulated during a cells life time, this supports a new hypothesis that nebulin assists in thin filament length regulation, not as a ruler (Reviewed in Littlefield and Fowler, 2008).

Nebulette has a molecular mass of ~100 kDa, so it is predicted to extend 150 kDa from the center of the Z-line (Moncman and Wang, 1995, 2000) which makes it unlikely to serve as a molecular ruler for cardiac muscle (Holmes and Moncman, 2008).

Similarities between nebulin and nebulette

Nebulin and nebulette share a 70% sequence homology and have highly similar domain layouts. The primary structures of these two proteins were analyzed to define the structurally important features in relation to the Z-line architecture (Moncman and Wang, 2000). They found that a partial cDNA corresponding to chicken adult nebulette

was found to be composed of nebulin-like 35 residue modules. Characterization of nebulette amino-acid sequence demonstrates that nebulette shares extensive sequence homology with the C-terminal portion of nebulin and also exhibits a four domain layout with high similarity to that of skeletal muscle nebulin (Moncman and Wang, 1999). Both nebulin and nebulette contain large domains composed of 35 residue modules; the motif is repeated 22/23 time in human nebulette and over 185 times in human nebulin (Moncman and Wang, 2000). In addition to the similar domains, nebulin and nebulette contain a linker and Src 3 homology at their C-terminal(Moncman and Wang, 2000). Figure 1 illustrates the homologous structure between nebulin and nebulette.

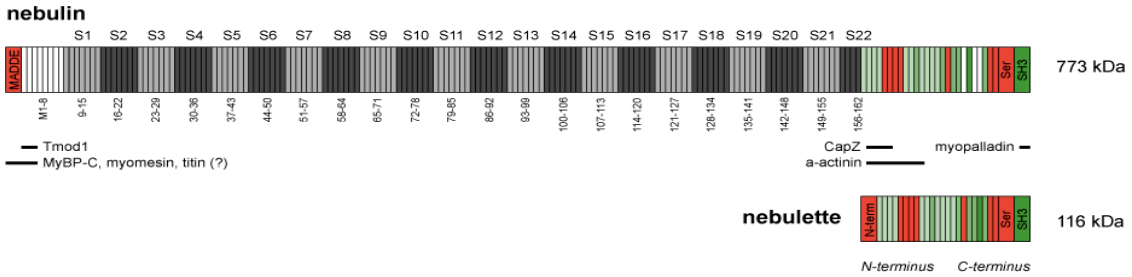

Figure 1: *Domain organization of nebulin and its cardiac isoform nebulette*. Nebulette reveals a four-domain layout similar to skeletal muscle nebulin. There is a short, acidic N-terminal, followed by 22 nebulin like repeats that are linked to a C-terminal Src homology 3 (SH3) via a short linker domain (Holmes and Moncman, 2008).

Some scientists speculate that the likelihood of nebulette having the identical functions in cardiac muscle as nebulin in skeletal muscle is not probable due to its smaller size. The fact that nebulette has been shown to interact with thin filament components in cardiac muscle, supports the notion that it may perform have some common functions with nebulin (Holmes and Moncman, 2008).

Research focus and hypothesis

Our research interest is the connection of desmin to the sarcomere and its effect on myocyte function during normal and disease. Previous experimental findings have concluded that desmin binds to nebulin, and have reported that desminopathy associated desmin mutation E245D increases binding to nebulin and perturbs actin thin filament architecture (Conover *et al.*, 2009). This is the first example of an intermediate-protein associated protein (IFAP) nebulin that has a dramatic structural effect on actin thin filaments in a desminopathy caused by a desmin mutation. Interestingly, this particular desmin mutation E245D forms seemingly normal filaments *in vitro* (Bar *et al.*, 2005b), suggesting that the molecular defect present in this case may indeed be caused by the inability of the contractile apparatus to communicate with the intermediate filament network (Conover *et al.*, 2009). Together, these findings are the basis to propose our hypothesis for this thesis that nebulin mutations associated with nemaline myopathy, located in nebulin modules that are known to date to be within modules that interact with desmin, could result from alterations in binding of nebulin to the desmin in skeletal muscles.

CHAPTER II

METHODS AND MATERIALS

His-tag and GST-tag affinity protein purifications were performed to prepare desmin and nebulin proteins used in GST pull down experiments and ELISA assays. A Bradford assay was performed on dialyzed His-tag proteins to determine their concentrations for GST-pull down and ELISA assays. The concentration of the protein is needed in order to determine the correct molar rations for the amount of GST-beads to His-tag protein in the GST-pull down and the nM concentration of proteins to be used on plate and in solutions for ELISA assays.

Bacterial protein inductions

On day 1 the bacterial colony is added from a culture plate to 40ml of 2xYT media and 40µl of the appropriate drug selection; Ampicillin (25ug/ml) for GST-Nebulin fragments and Kanamycin (50ug/ml) for His-Nebulin fragments. *E. coli* bacteria BL21 strain grows overnight in a shaker at 37^{o}C. The next day, the overnight culture is transferred to a larger flask with 800ml 2xYT media and 800µl of the appropriate drug selection. The culture continues growing for 90 minutes, at this time an OD_{600} reading is taken along with a 1ml gel sample. The goal is to get the reading as close as possible to 0.600, to ensure that the bacteria is just entering the log phase of bacterial growth. Once the OD_{600} reaches this level 0.5M IPTG is added to the flask and the culture is induced for 3-4 hours. After this time another OD_{600} is taken along with a 1ml gel sample. The rest of the

culture is spun down in a centrifuge at 5000 rpms for 10 minutes. The resulting pellet is frozen at -20^{o}C until it used for affinity purification.

His-tag affinity protein purification

The His tagged nebulin fragment pellets are resuspended with 10ml lysis buffer (list composition) and 200µl of protease inhibitors (Sigma). After resuspension the pellets are homogenized 3 times each by dounce homogenization, 10 plunges each time. This provides a mechanical lysing of the pellets. The next step is to centrifuge the dounce homogenized pellets at 15000 rpms for 45 minutes to achieve a clear soluble lysate. While the pellets are centrifuging, Ni-NTA beads need to be rinsed to remove the EtOH in the storage solution. This procedure is repeated 3 times to completely clean the beads. 400µl of Ni-NTA beads and 400µl of lysis buffer in an eppendorf that is centrifuged at 14,000 rpms for 1 min. The clear lysate is separated from the centrifuged pellet and placed in a labeled 15ml conical with 400µl of clean beads. The conical are incubated overnight at 4^{o}C on a tube rotator.

The next day, batch purification of the lysate and bead mixture is performed. Disposable 15mls columns are used for all the washes and elutions. The wash buffer (100nM NaH_2PO_4, 10nM Tris-Cl, 8M urea; pH to 6.3) is a mixture of 250ml wash buffer and 2.5ml Triton X-100. The protein and bead mix is transferred to the disposable column and the flow through is collected into a clean 15ml conical, this samples constitutes the unbound lysate.

The next step is to wash the beads with 10ml wash buffer plus1% Triton X-100, 3 times. The flow through is collected in a separate conical after each wash. The last step is to elute the beads with 0.3ml of elution buffer (100nM NaH_2PO_4, 10mM Tris-Cl, 8m urea; pH to 4.5) is added to the column and 0.5ml is collected in consecutive labeled eppendorfs (elution 1-6). The success of the purification is evaluated by SDS-PAGE. Several gel samples are collected: 40µl of each elution unbound lysate, all three washes and a bead sample after elutions were collected; 80µl 3X lamelli buffer is added to each gel sample. Samples are boiled prior to loading into the SDS-PAGE gel. To examine the elution gel samples 20µl each are used plus 40µl 3X lamelli buffer. The gel in figure 2 is an example of the elutions taken from purification. Figure 2 also has a flow chart illustrating the steps previously described in this section. The flow chart provides a basic outline for the procedure that can be modified as needed.

A.

His-Tag Purification Flow Chart

Thaw the induced pellet on ice for 15 minutes

↓

Add 10ml lysis buffer and 200ul protease inhibitors; resuspend the pellet by vortex

↓

Sonicate the lysate mixture 3 times, ten bursts each time

↓

Dounce homogenize lysate mixture 3 times, ten plunges each time

↓

Centrifuge the lysate for 30 minutes at 15000 rpms

↓

Add 1ml of the 50% Ni-NTA slurry to the cleared lysate and mix gently by rotating at 4°C overnight

↓

Load the lysate/Ni-NTA mixture into a column with the bottom outlet capped

↓

Remove the bottom cap and collect the column flow through

↓

Wash 3 times with 10ml wash buffer; collect each wash flow through and collect fractions for SDS-PAGE analysis

↓

Elute the protein 6 times with 0.5ml elution buffer. Collect the eluate in 6 tubes and analyze by SDS-PAGE

B.

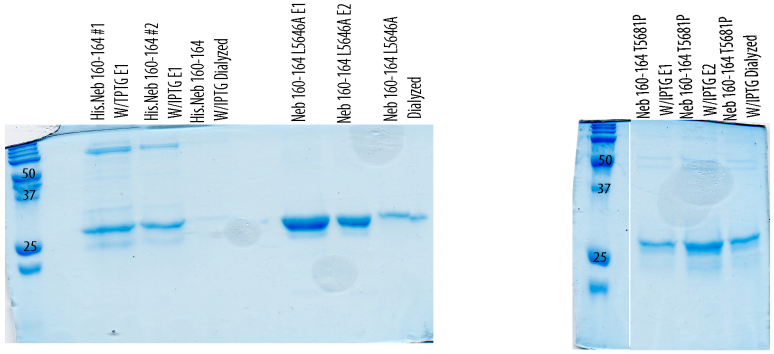

Figure 2: *His-tagged purified proteins analyzed by SDS-PAGE electrophoresis.* **(**A) Flow chart for His-tag purification details individual steps required for the affinity tag purification. (B) SDS-PAGE gels pictured are of His-Nebulin 160-164 Wild type, Nebulin 160-264 T5681P and Nebulin 160-164 L5646A purification samples before and after dialysis into binding buffer was performed. The concentrations of each protein were determined using the OD600 values obtained in the Bradford assay. These gel samples correspond with the concentration values I calculated. The abbreviations on the gel correspond to E1-elution 1, E2-elution 2, and D-dialyzed.

GST-tag affinity protein purification

The pellets are resuspended with 25ml of 1X PBS/ 1% Triton X-100 plus 200µl of protease inhibitors (Roche). Once the pellets have been resuspended, 0.5ml of 1mg/ml chick embryo lysozyme is added, and then the solution sits on ice for 30 minutes. During this time the glutathione beads are rinsed, by adding 500µl of beads and 500µl of 1X PBS to an eppendorf and centrifuged 14000 rpms for 1 min. The supernatant is discarded and 500µl of 1X PBS is added. The procedure is repeated three times to ensure that the beads are clean of their storage solution. After 30 min, the pellets are sonicated 3 times each, with ten bursts each time with a 1min rest between sonication always keeping the samples on ice. After sonication, the samples are dounce homogenized 3 times each, with ten plunges each time on ice. The bacterial lysate is then centrifuged at 15,000 rpms for 45 min, and the resulting clear lysate is pipetted into a 15ml conical mixed with 500µl of glutathione beads. The bead and lysate mixture is rotated at 4^{o}C for 90 minutes.

Once this time is done, the conical is centrifuged at 3000 rpms for 5 min and the supernatant is removed, this is the unbound lysate. 10mls of wash buffer (1X PBS/ 1% Triton) is added to the beads to remove non-specific proteins binding. The mixture is centrifuged at 3000 rpms for 5 min. The beads are stored at 4^{o}C until needed for pull-down experiments. Several gel samples are collected: 40µl post-dounce homogenized sample, a 40µl clear lysate sample, a 40µl wash sample and a 40µl bead sample. 80µl of 3X lamelli buffer are added to each sample and analyzed on a SDS-PAGE gel that is stained with Coomassie brilliant blue to visualize the proteins.

Bradford assay

The Bradford assay is used to estimate the concentration of proteins to be used subsequently in biochemical assays. Affinity purified proteins are dialyzed ON into binding buffer (80mM KCl, 20nM HEPES, 2mM $MgCl_2$; pH to 7.4) or 1X PBS. These concentrations are used to determine the amounts of dialyzed protein that will be used in ELISA assays and pull down experiments. There are 3 controls that need to be used for the Bradford assay: BSA stock, dye, and binding buffer. The assay is performed by a series of dilutions of the target proteins and BSA standard in a 96 well microtiter plate. The first dilution of BSA standard is 250ug/ml, each dilution after that is one half of the previous dilution until 1.8ug/ml is reached. The dilutions are made by taking 500µl of the previous concentration and adding 500µl of binding buffer to reduce the concentration by one half.

The protein dilution is different because the concentration of the protein is unknown. For these dilutions, 50µl of protein to 270µl of binding buffer for the first well, this is a dilution of 0:0. From there 160µl of the first dilution is taken out an added to 160µl binding buffer to create a 1:2 dilution. This step is repeated until a dilution of 1:128 is reached. Once all the dilutions have been performed, 160µl of each dilution is added to its respective well. To each well 40µl of dye is added and the plate is left at room temperature for at least 5 minutes but no longer than one hour. The concentration of each protein is measured with an Omega plate reader, which gives an absorbance level in OD_{595}. From this OD_{595} reading, along with a standard curve graph; seen in Figure 3,

and the concentration of each unknown protein tested is estimated based on a linear regression of the BSA standard.

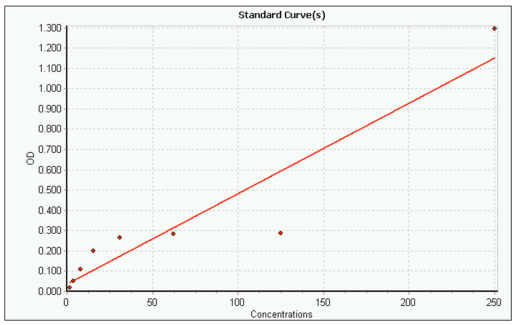

Figure 3: *Bradford assay.* The standard curve shown depicts a BSA standard curve. A OD_{595} absorbance was used to calculate the concentration of each protein. In this assay, the concentration of the following fragments was estimated: His-nebulin 160-164 WT is 0.312ug/ml, nebulin M160-164 T5681P is 0.584ug/ml, and Nebulin 160-164 L5646A is 0.490ug/ml. The fit of the graph represents the absorbance levels of the tested proteins at 405nm. An R-value of 0.88 . This value corresponds to the slope of the linear fit of the known dilutions for BSA. Triplicate well were performed the mutants, T5681P and L5646A; and duplicate sample were performed for the WT protein. These concentrations were used to plan the GST-pull down experiment.

GST-pull down assays

The GST-pull down is used to determine the capacity of GST-tagged desmin fragments to associate to His-nebulin protein fragments. The amount of protein used is dependent on the concentration of His-nebulin proteins and the estimated amount of GST-desmin protein present in the glutathione beads from the GST-desmin purification. Based on SDS-PAGE analysis of GST-protein/bead slurry and the protein concentration of the nebulin fragment a determined amount of each protein is mixed in a 1.5ml tube. The beads are washed twice with 100ul of binding buffer (or 1x PBS)/ 0.1% Triton, and spun for 2 min at 3000 rpms for each wash. After the washes the His-nebulin fragment previously dialyzed into the appropriate buffer is added to the GST-nebulin bead/protein. The final volume of the eppendorf is brought to 100ul and it is incubated for one h in a small tube rotator at 4^{o}C.

After incubation, the bead / His-nebulin mixture is washed 5 times with binding buffer (or 1x PBS)/ 0.1% Triton, with two min at 3000 rpms in a centrifuge for each wash. Once the washes are complete, 70ul of 3 X lamelli buffers is added to the beads and analyzed on a 15% SDS-PAGE gel. There will be control beads for each gel; these consist of clean glutathione beads that have gone through the pull-down process, except that no proteins have been added. Since the bound protein pairs will coprecipitate both samples, this ensures that the size of each protein is compared from the control samples.

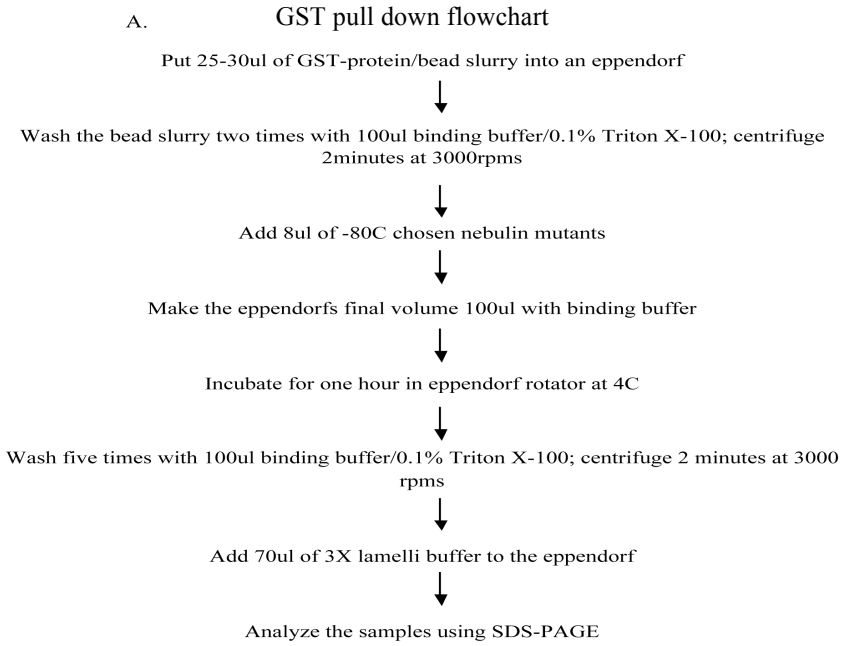

Figure 4: *GST pull down procedure.* The pull down experiment flow chart is an overview of the steps for this procedure. Minor adjustments to the procedure have been made depending on the starting materials, for example, the amount of GST-protein/bead slurry used or using 1X PBS buffer instead of binding buffer. These changes are to be expected since they are based on the buffer used in dialysis and purification and the concentrations of the His-nebulin proteins being used at the time.

ELISA binding assay

The ELISA (Enzyme-linked immunosorbent assay) plate is coated with 40nM of Nebulin fragment (in binding buffer 20mM Hepes pH 7.4, 80mM KCl, 2mM $MgCl_2$) for

endpoint ELISAs and 50nM Nebulin fragment for Saturation curves per well in 100µl total volume in 0.1M Carbonate buffer pH 9.6 (3.43g sodium bicarbonate + 0.97g sodium carbonate in 500ml H_2O; pH with NaOH) and left at 4^oC overnight. For each saturation curve ELISA control wells were also included as part of the experimental design. These wells were the nebulin fragment with no protein in solution only BSA in the buffer, recombinant GST-protein alone with BSA,d and carbonate buffer with no protein added on the plate or in solution. The next day, the wells need to be washed 4 times with binding buffer/ 0.05% Tween/ 0.5%BSA. After washing, the wells are blocked for 30 min with binding buffer/ 0.2% BSA/ 0.05% Tween at 4°C. After 30 min, 100nM of biotinylated coil 2b and GST control in binding buffer/ 0.2% BSA/ 0.05% Tween is added to each well and incubated at RT for 1h. The wells are once again washed 4 times with binding buffer/ 0.05% Tween/ 0.2% BSA. Next, the wells are incubated with ImmunoPure Strepavidin antibodies(Pierce), diluted to 1:20000 in binding buffer/ 0.05% Tween/ 0.2%BSA, for one h at RT.

After this incubation, the wells are washed 4 times with binding buffer/ 0.05% Tween/ 0.2% BSA. Then pNPP substrate (Sigma N-9389) was added at 1mg/ml in Substrate buffer (0.1 M glycine, 1mM $MgCl_2$, 1mM $ZnCl_2$; pH to 10.4 with NaOH). The plate was incubated at 37°C for 30 min. The plate was read at 405nm using Omega spectrophotometer plate reader. The layout of the plate is specified on the machine before reading. Once the absorbance values are obtained, we can plot a curve and estimate the affinity constant for a pair of binding proteins. Figure 5 shows the layout of

the ELISA plate and a graph that illustrates the binding affinity of the nebulin fragments to GST-alone and GST-coil 2b.

Western blot analysis

Western blots were used to detect specific proteins within a given sample. In our experiments, we attempted to detect His-tagged nebulin proteins. The samples are run on a SDS-PAGE gel at 150V for 1 h and 30 min. The proteins in the gel are transferred to a nitrocellulose membrane using an electrophoretic transfer box and a methanol based transfer buffer (20nM Tris, 150nM Glycine, 20% Methanol). The transfer was performed for 1 h at 100V or ON at 30V at 4°C. Once the transfer is completed, the membrane is stained with Ponceau-S stain for 5 min, then it is rinsed with distilled water. The membrane is blocked in 1X PBS/ 5% milk for 1 h. The blocking step ensures that the antibody attaches only to the target protein by saturating unoccupied binding sites with BSA present in the milk. Once the blocking step is complete, the membrane can be probed with the desired antibody. In our experiments, we use two different antibodies; a monoclonal His-HRP conjugated antibody, which binds to His-tagged proteins, and polyclonal rabbit nebulin M160-164 antibodies, which specifically binds to the 160-164 region of nebulin which are subsequently incubated with secondary anti-Rabbit HRP antibodies.

For the His-antibody Western blot analysis, we use 10ml of the milk and approximately 1:2000 dilution of the antibody. This mixture is used to cover the membrane and gently shaken at RT for 1 h. The membrane is washed 4 times with 1X PBS/ 0.05% Tween,

using 10ml for each wash. Once the washes are finished the membrane is developed. To do this, we place the membrane between two protector sheets in the cassette. To the membrane we add a mixture of 200ul SuperSignal® West Pico Stable Peroxide and 200ul SuperSignal® West Pico Luminol/Enhancer solution, this mixture allows the film to pick up the fluorescent tags of the secondary HRP antibody that has bound to the target protein. In a dark room, the film is exposed for 1min, 10 min and ON if needed. Once we are finished with developing the membrane we can strip it and add a new antibody to detect the GST-proteins on the membrane.

To strip the membrane of the first antibody we use 0.1M Glycine buffer pH 2.5, 1X PBS, and 1M NaCl in PBS. The first step is to strip the membrane at RT with 10ml 0.1M Glycine buffer for 15 min. Next the membrane is washed with 1X PBS for 10-15 min. This is followed by 1M NaCl in PBS for 15 min and another wash with 1X PBS for 10 - 15 min. After the membrane has been stripped; the normal steps for Western blotting, starting with blocking in 5% milk, are repeated. The new antibody uses a two step process. After the membrane has been blocked the primary antibody, anti- nebulin M160-164 rabbit antibody, was added, approximately at a 1:5000 dilution in 1X PBS/ 5% milk, to the membrane for 1 h at RT. After the secondary antibody goat anti-rabbit IgG is added at 1:20000 dilution in 1X PBS/ 5% milk, the membrane is incubated for 1 h at RT. Finally, the washes are performed and the membrane developed in a similar manner as described above.

CHAPTER III

RESULTS

Recent published results showed that the non-mutated WT nebulin modules 160-164 bind with a high affinity to the coil 1b region of desmin (Conover *et al.*, 2009). In this Thesis, we used a nemaline-myopathy associated mutant -nebulin M160-164 T5681P-, and a control mutant in the same region -nebulin 160-164 L5646A- to investigate its binding properties to different regions of desmin intermediate filaments. Through GST-pull down and ELISA assays we have determined whether these mutant proteins bind to desmin, to assess in future studies whether these binding interactions might result in architectural alterations in the overall binding of desmin intermediate filaments linkage to the sarcomeres by the thin filaments via nebulin.

Desmin coil 2B region binds Nebulin mutant M160-164 L5646A

It has been shown that desmin binds to nebulin module M160-164 through ELISA assays (Conover *et al.*, 2009). In this Thesis, we show that desmin coil 2b binds to WT nebulin M160-164 and to its L5646A mutant through GST-pull down experiments, as illustrated in Figure 5. To verify these results, we used a Western blot analysis on the samples probed with specific anti-nebulin M160-164 antibodies. This allowed us to verify that the bands seen with GST-coil 2B in the gel were nebulin M160-164. The film is shown in Figure 5 along with the Ponceau-S staining of the same membrane.

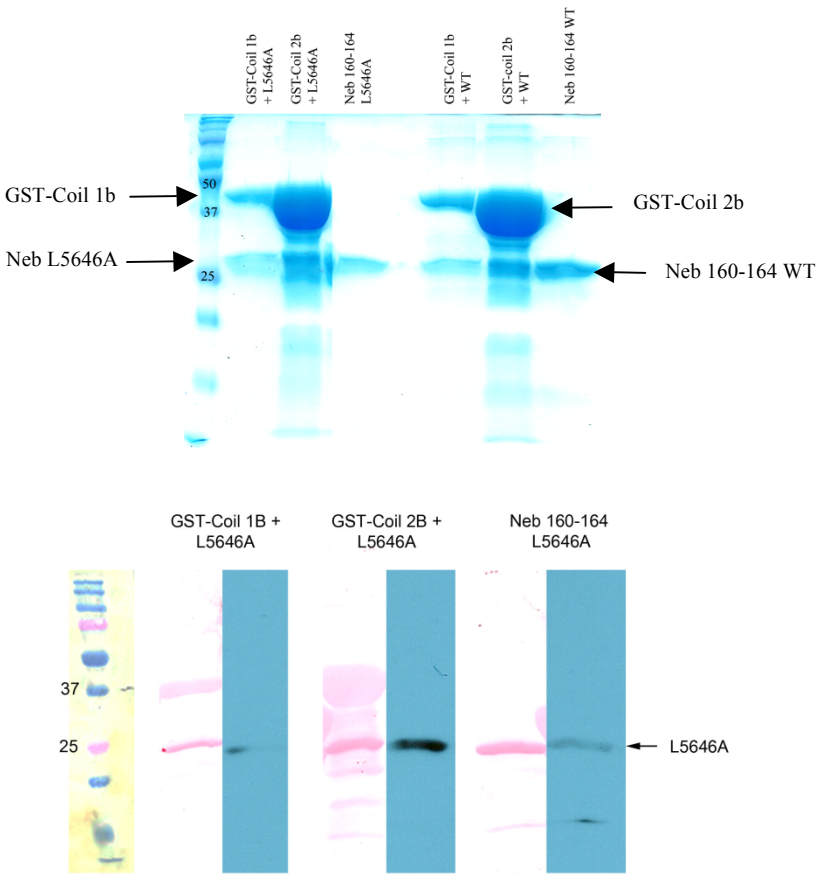

Figure 5: *GST pull down experiment of His tagged nebulin fragments with GST-coil 1B and 2B along with Western blot analysis of the samples.*
The fragments show that both WT and mutant L5646A nebulin M160-164 are capable of binding both alpha-helical desmin central coil 1B and 2B fragments. (A) GST-pull down assays show that GST-coil 2b (42kDa) binds to the L5646A (27kDa) mutant and to GST-coil 1b domain (40kDa), the latter domain had been shown previously to bind very strongly to the wild type nebulin M160-164 (25 kDa). (B) The Western blot analysis of the samples verifies that nebulin mutant L5646A was pull-down with GST-coil 1B and GST-coil 2B coated glutathione beads.

Our GST-pull down results show that desmin's coil 2b binds as well to WT nebulin M160-164 to L5646A nebulin M160-164. ELISA assays were used to determine and compare the binding affinities (Kd) for the each of the nebulin fragments. Through ELISA assays we determined that the binding affinity of desmin coil 2b was much

weaker toward L5646A that it was to the WT nebulin M160-164. The data consistently showed a decrease (~5 fold) in binding of L5646A to coil 2b as compared to WT nebulin M160-164 protein. The affinity constants (K_{ds}) determined in experiment shown in Figure 6 are 10-fold different between the two samples. In particular, the lower K_d obtained for coil 2B binding to WT nebulin M160-164 suggests a stronger binding affinity as compared to that of mutant nebulin M160-164 L5646A. Both biochemical methods consistently showed that desmin coil 2b binds to both proteins, and revealed a lowered binding affinity (with an estimated Kd of 175.2 nM) to the mutant nebulin M160-164 L5646A as compared to WT protein that had an estimated Kd of 18nM. This data suggests that single missense mutations in nebulin are capable of altering the interaction between desmin and nebulin, which are expected to dramatically influence the sarcomere contractile function by decreasing the binding of the thin filaments to the extrasarcomeric desmin network.

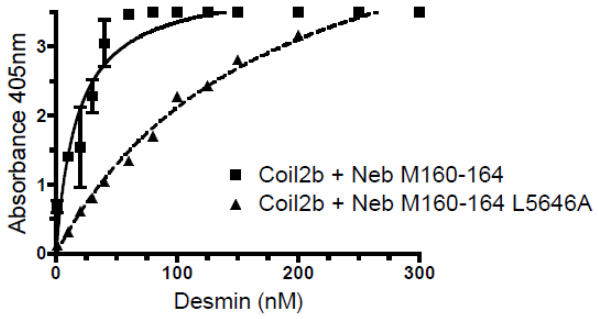

Figure 6: *ELISA assay shows the saturation curve of desmin coil 2b and WT nebulin M160-164 as compared to desmin coil 2b and nebulin M160-164 L5646A.* The nebulin fragments were plated at a concentration of 50nM on the microtiter plate and tested for binding with desmin coil 2B at different concentrations. The graph shows that desmin coil 2b binds to nebulin M160-164 with an estimated dissociation constant (K_d) of 18nM and a binding capacity (Bmax) of 3.9. In contrast, our results show that desmin coil 2b binds to the nebulin M160-164 L5646A mutant with a K_d of 175.2nM and a Bmax of 5.8.

Desmin coil 2B shows decreased binding to nebulin mutant M160-164 T5681P

The coil 2b region of human desmin spans amino acids (296-416); the tail region spans the region (417-470). The full-length desmin protein is 470 amino acid residues long. Our results showed that the tail region of desmin binds to the nemaline-associated nebulin mutant T5681P (Figure 7). Specifically, our pull-down experiment indicates that desmin GST-tail bound to nebulin M160-164 T5681P (data not shown). Our preliminary results showed no detectable binding of nebulin M160-164 T5681P to desmin coil 1B region by this method, in stark contrast to the high affinity binding interaction known to occur between WT nebulin M160-164 and desmin coil 1B (Conover et al. 2009). Ongoing ELISA experiments will determine the Kd for this association.

To further characterize of the binding capacity of nebulin M160-164 T5681P as compared to a random alanine mutant exchange in the same region L5646A we performed saturation curves ELISAs on the same plate testing these mutants for binding for both the coil 2b and tail regions of desmin (Figure 7). Our data shows nebulin M160-164 T5681P NM-associated mutant having an stronger binding affinity to tail (K_d of 63.1 nM) and to coil 2B (K_d of 34.4 nM) as compared to nebulin M160-164 L5646A mutant (tail K_d of 170.8 nM; coil 2B K_d of 167.1 nM). This results indicate that each mutant has differential the binding properties to different parts of desmin.

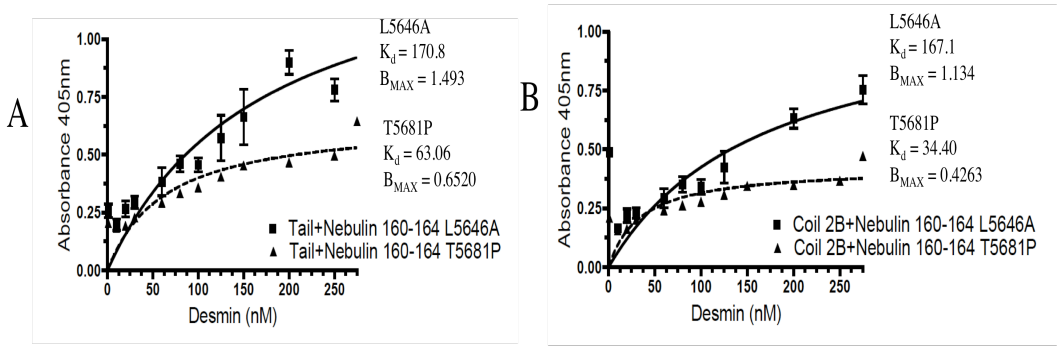

Figure 7: *ELISA saturation curves of Neb160-164 L5646A vs. Neb 160-164 T5681P with GST-tail and GST-coil 2B.* (A) ELISA saturation curve of L5646A vs. T5681P with GST- tail. This plate illustrates the difference in binding for the mutants to GST-tail. It can be seen that T5681P binds stronger to GST-tail with a K_d of 63.06 and a B_{max} of 0.6520. (B) ELISA saturation curve of L5646A vs. T5681P and GST-coil 2B. This plate shows the difference in binding between the two mutants to GST-coil 2B. It shows T5681P having the stronger binding with a K_d 34.4 and a B_{max} 0.4263. These results support earlier data showing T5681P to have a greater affinity to coil 2B over L5646A.

Our data revealed that this nemaline-myopathy associated nebulin mutant bound to desmin GST-coil 2b region with a 5-fold decrease in affinity with respect to the WT His-nebulin M160-164 fragment (Figure 8). In accordance to our previous saturation curve (Figure 6), our results show high affinity binding for coil 2B to WT nebulin M160-164 with an estimated K_d of 34 nM (Figure 8). In contrast, the nemaline myopathy mutant nebulin M160-164 T5681P showed a lowered affinity binding with an estimated K_d of 175nM when tested for binding with desmin coil 2b.

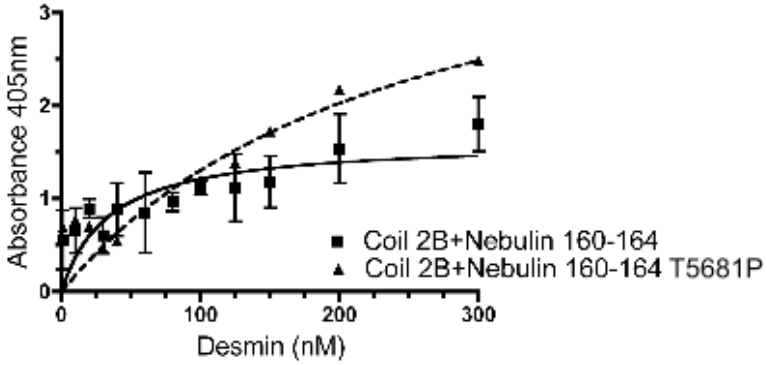

Figure 8: *ELISA assay shows the saturation curve of desmin coil 2b and wild type nebulin M160-164 as compared to desmin coil 2b + nebulin M160-164 T5646P.* The nebulin fragments were plated at a concentration of 50nM on the microtiter plate and tested for binding with desmin coil 2B at different concentrations. The graph shows that desmin coil 2b binds to nebulin M160-164 with an estimated dissociation constant (K_d) of 34nM and a binding capacity (Bmax) of 3.942. In contrast, our results show that desmin coil 2b binds to the nebulin M160-164 T5681P mutant with a K_d of 249.1 and a Bmax of 4.549.

Desmin tail region exhibits low affinity binding to Neb M160-164 T5681P

Ongoing experiments aim to determine the dissociation constants for the interaction of desmin GST-tail domain and both nebulin M160-164 mutants L5646A and T5681P.

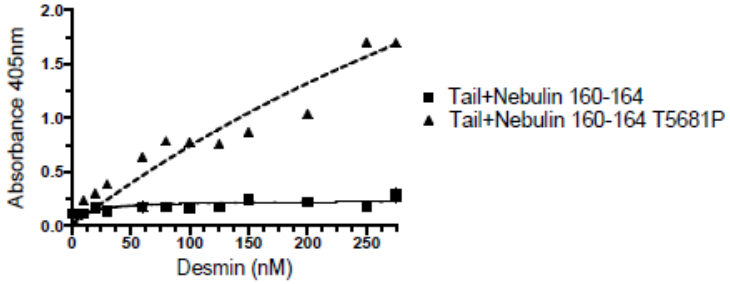

Figure 9: *ELISA saturation curve assay illustrating GST-tail binding to WT and T5681P.* This saturation curve shows the binding profile differences to tail for WT and T5681P. The estimated K_d values for T5681P to tail is 738.5 nM and for WT to tail it is 12.1 nM . These values show the WT having a higher binding affinity for desmin tail as compared to nebulin M160-164 T5681P.

Further research will likely show that T5681P nebulin M160-164 mutant alters the binding of nebulin to desmin in muscle sarcomeres causing significant effect on actin regulation, we predict that this knowledge may help explain the molecular causes some of a number of clinical symptoms problems seen in nemaline myopathy patient cases.

Nebulin M177-181 binds to GST-tail and GST-coil 2B domains of desmin

We know from previous research that nebulin M160-164 fragment binds to the GST-coil 1B domain of desmin (Conover *et al.*, 2009). We wanted to test if other modules closer to the C-terminal of nebulin near the Z-disc in the sarcomere also had the capacity to bind to particular desmin fragments. Both ELISA endpoint and saturation assays determined that nebulin M177-181 binds to GST- tail and GST-coil 2B regions of desmin (Figure 10). Moreover, our results show that the binding of WT nebulin M177-181 to the tail region of desmin is stronger than the binding for M160-164 WT; this can be seen in figure 10.

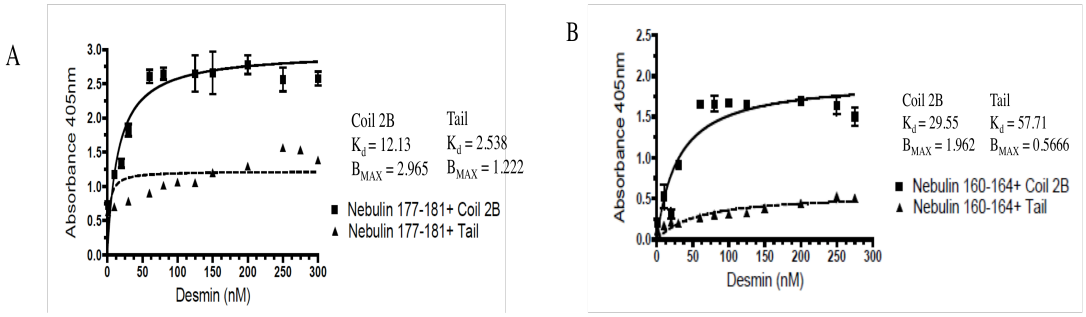

Figure 10: *ELISA saturation curve of GST-coil 2B Vs. GST-tail with His-tagged nebulin 177-181 and His-nebulin 160-164.* These graphs illustrate the difference in binding affinity (Kd) and capacity (Bmax) of WT nebulin 177-181 and WT nebulin 160-164 WT to desmin GST-coil 2B and desmin GST-tail. (A) The binding capacity of the nebulin WT module 177-181 to coil 2B and tail. Nebulin M177-181 binds with high affinity to tail (K_d is 2.538) as compared to desmin coil 2B with a K_d of 12.13. (B) The opposite trend is seen in the graph showing the binding of WT nebulin M160-164 to desmin GST-coil 2B (K_d is 29.55) and GST-tail (K_d is 57.71). This experiment is courtesy of Samaneh Karami.

To validate our results we ran a Saturation Curve ELISA to ensure that the Desmin proteins where binding to the nebulin fragments and not the GST. The ELISA was set up with the nebulin fragments and coated with GST-alone as the secondary protein. The absorbance values from this ELISA (Figure 11) ensured us that GST is not the cause for the binding seen in earlier ELISAs.

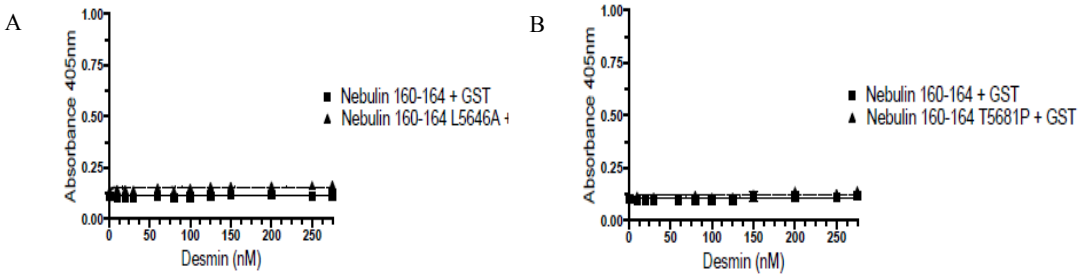

Figure 11: *ELISA saturation curves of Neb 160-164 WT vs. L5646A & T5681P with GST-Alone.* The ELISA graphs demonstrate the effect of GST-Alone on binding to Nebulin fragments. The K_d values determined for binding between Nebulin fragments and GST-Alone are very small and insignificant when compared with K_d values from GST-Desmin ELISAs. (A) GST-Alone shows no significant binding for neb 160-164 WT and L5646A; the K_d for L5646A is 0.141, for WT it is 0.07559. (B) There is no significant binding seen between GST-Alone and Neb 160-164 T5681P; the K_d value is 0.2057 for T5681P and 0.03439 for WT.

CHAPTER IV

SUMMARY AND CONCLUSIONS

Discussion

Mutations in six different genes have been found to cause nemaline myopathy (NM) in humans, a non-dystrophic myopathy. The majority of mutations are thought to occur in nebulin, while other genetic causes for NM include mutations other sarcomere proteins such as tropomyosin-3 (NEM1), alpha-actin-1 (NEM3), beta-tropomyosin (NEM4), troponin T1 (NEM5), and cofilin-2 (NEM7). The chromosome site for NEM6 has been mapped but no genetic locus has been identified to be linked to the disease. Historically, the large size of nebulin protein has hindered the search for NM causative mutations within the nebulin gene (Pelin *et al.*, 1999).

Recent functional studies in a NM case caused by a small deletion in nebulin exon 55 have shown that muscle weakness may result from deregulated thin filament as this muscle exhibits reduction of 60% force generation (Ottenheijm *et al.*, 2009). However, little is known of the contribution of the intermediate filament system to the force generation activity of the sarcomere. Since previous research initially showed that the giant nebulin protein bound to desmin by yeast-two hybrid analysis (Bang *et al.*, 2002) and other data established that WT nebulin M160-164 had a high binding affinity for the desmin coil 1B region (Conover *et al.*, 2009), we reason that given the importance of desmin to the force generation ability of muscle, if we found alterations of binding

between these molecules in NM it may provide for elucidating the functional basis of muscle weakness in NM. Thus, for this Thesis research, we focused our investigation on the nemaline-associated mutation T5681P to test whether our hypothesis was correct and elucidate how a known NM mutation (Pelin *et al.*, 2002) would affect binding to desmin. We know that nebulin binds to desmin at M160-164 to desmin coil 1B, thus we choose a mutation within M160-164 region to characterize the potential binding difference profiles between the WT and the mutant.

Interestingly, this particular nebulin mutation T5681P was found in two affected children in one Finnish family and in a single patient from another Finnish family. This study was done in 2002, with 77 individual patients with various forms of nemaline myopathy. The clinical symptoms observed in the patients with the T5681P mutation varied between typical (one sibling and the single patient) and intermediate (the other sibling) forms. Typical symptoms include moderate muscle weakness in face, trunk and limb muscles. Intermediate symptoms are more severe. The mutation is a missense mutation in exon 160 which changes threonine to proline (T5681P) (Pelin *et al.*, 2002). Based on these clinical findings we proposed a hypothesis that mutations in the C-terminal part of the nebulin gene near the Z-disc associated with NM could result from alterations in binding of nebulin (or potentially other nebulin family members) to the desmin.

In our research we also studied a random alanine exchange mutation, M160-164 L5646A, to compare our binding results to a non-pathogenic mutation within the same region that the nemaline-myopathy mutation, and better understand the specific effects caused by the disease-associated nebulin T5681P mutation. Interestingly, the L5646A mutation is more N-terminally located compared to T5681P (35 residues). Our results show differential binding between nebulin M160-164 L5646A and the T5681P mutant since we observed a lower binding of the non-pathogenic control mutant to desmin coil 2B (Figure 7).

Nebulin M177-181 binds to desmin tail region

To gain further insight on the type of residues present in nebulin modules that are critical for the interaction of nebulin and desmin, we tested whether other more C-terminal modules M177-181 from modules M160-164 were involved in the interaction with desmin. Motivated by previous yeast-two hybrids studies that showed positive interaction of a nebulin M160-183 with full-length desmin but that lacked the variably spliced modules M177-181 from psoas muscle (Bang *et al.*, 2002), we tested whether these modules would contained type of residues required for a productive interaction. Contrary to expected results, our results showed that nebulin M177-181 does bind to desmin at the tail region. It also appears to bind to the coil 2B region, but not as strongly as M160-164 (Figure 10). These results suggest that multiple binding sites for desmin are present within nebulin C-terminal end that have differential binding affinities. The significance of these findings warrants further investigation.

Desmin coil 2B and coil 1B regions exhibit binding to nebulin mutant L5646A

Our results revealed that a random alanine substitution mutant nebulin M160-164 L5646A binds to desmin coil 1B and coil 2B regions with a lower binding affinity than to WT nebulin M160-164. This allowed us to have a base reading for future testing with nemaline- associated nebulin M160-164 T5681P mutant.

Our results also revealed that nebulin M160-164 T5681P mutant binds with significantly lowered binding affinity (~14 fold lower) than random nebulin M160-164 L5646A to desmin's coil 2B (~10 fold lower) as compared to wild-type nebulin M160-164 (Fig 6 and 8). The lowered binding affinity may indicate a weaker association between desmin coil 2B region and mutant T5681P within cells preventing/ modifying normal sarcomere contraction. This weakening may aid in explaining the clinical symptoms observed in muscle from patients carrying the recessive T5681P missense mutation seen at exon 160 in the nebulin protein (Pelin *et al.*, 2002).

Nebulin mutant M160-164 T5681P binds to desmin coil 2B and tail regions

Our ELISA saturation curves analysis show that nebulin M160-164 T5681P NM-associated mutant binds with a higher binding affinity to desmin coil 2B (~5 fold higher) and tail (~3 fold higher) domains as compared to nebulin L5646A mutant (Figure 7). The tail domain of desmin is the non α-helical carboxyl-terminal end of desmin. Recent research has shown that the tail region is important in setting up the mechanical filament

properties of desmin (Bar *et al.,2010*). Our data reveals that nebulin M160-164 T5681P has a different alternative binding site to desmin at its tail region which it binds with low affinity (738.5 nM) in contrast to what was found for WT nebulin M160-164 (Fig 9). These results show that mutant T5681P has a dramatic impact on desmin domains than the mutant nebulin M160-164 L5646A, which may cause decoupling of thin filament system from the intermediate filament network. This finding supports our hypothesis that NM associated nebulin mutations can alter the binding of nebulin to desmin *in vitro*.

Outlook and future research directions

We proposed that the association of desmin intermediate filament network to the sarcomere plays a pivotal role in nemaline myopathy caused by nebulin mutations. In this work, we showed by two independent biochemical approaches that the interaction of desmin with nebulin is not restricted to one binding sites but rather is complex and occurs via multiple regions in each molecule. Additionally, we showed that altered binding affinity is displayed by nemaline-associated nebulin M160-164 T5681P mutant as compared to non-mutated nebulin and to a random nebulin L5646A mutant. Another interesting result that we obtained was finding a new binding site between desmin tail and nebulin at M177-181(nebulin) (Figure 10, unpublished data S. Karami and G. Conover). Our future experiments will continue testing and characterizing for new binding sites within nebulin and other nebulin family members, nebulette to desmin domains. Taken together, our results support our hypothesis that alteration of nebulin association with desmin may be responsible some of the symptoms observed in NM

patients. Further investigation using *in vivo* animal models is warranted to further support our findings.

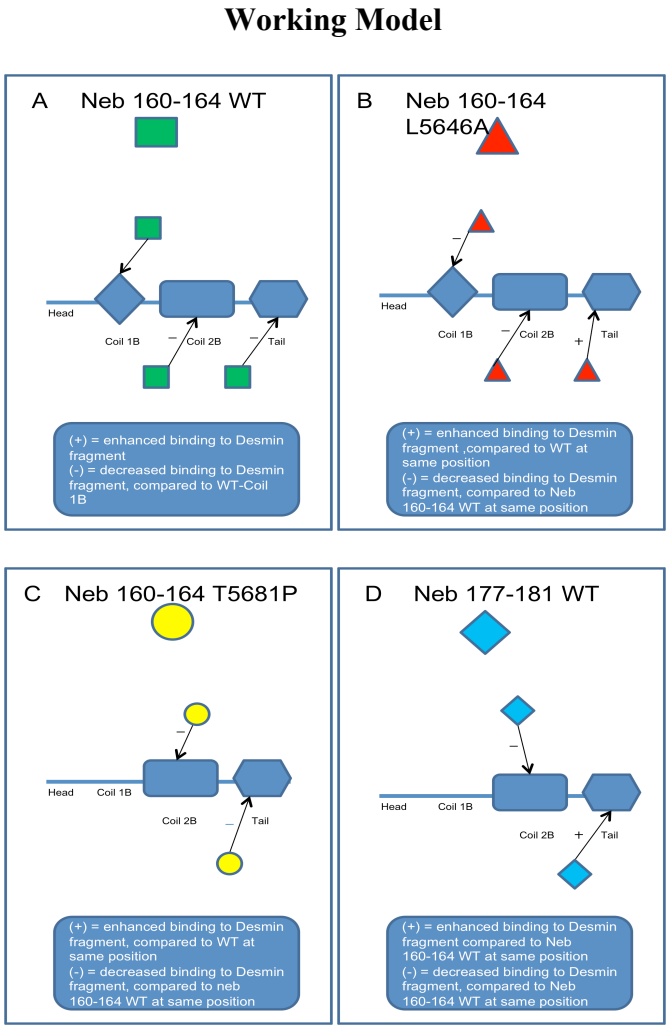

Figure 11: *Working model of nebulin M160-164 WT and mutants and M177-181 WT binding to desmin.* This figure illustrates the binding sites that we have identified through our research. Each WT or mutant has been seen to binds to two different areas of desmin. The arrows illustrate where each fragment has been seen to bind. It also shows the increase (+) or decrease (-) in binding as compared to the WT fragment at the same position. (A) This shows the sites on Desmin the M160-164 WT binds to. The (+) and (-) symbols show the increase or decrease in WT binding as compared to WT and coil 1B (Conover et al. 2009), which is the original site identified for WT and desmin to bind. (B) The model shows the binding sites for L5646A to desmin. (C) The last figure shows the binding sites we have found for T5681P to desmin. (D) This model depicts the binding between desmin and nebulin for Neb M177-181.

Since desmin is abundant in both skeletal and cardiac muscles, we propose that most likely a number of nebulin mutations associated with disease could be relevant to events occurring in cardiac muscle cells. However, since nebulin is found in low levels in cardiac muscles (Kazmierski *et al.*, 2003), we propose that the nebulin isoform nebulette, containing significant homology to the C-terminal end, and that is found in high levels in cardiac muscles (Moncman and Wang, 1995), may constitute the link that binds desmin to nebulette in cardiac muscles forming part of the intermediate filament continuum and transmitting lateral and longitudinal intermyofibrillar force between muscle cells.

Desmin interacts with nebulin establishing a direct link between the interfilament network and sarcomeres at the Z-discs (Conover *et al.*, 2009). This interaction between nebulin and desmin, and previous published results that show nebulin and nebulette have homologous interactions with thin filament structures, leads us to propose that the same interaction could be possible between nebulette and desmin in cardiac muscle. Future investigations aim to discover whether nebulette has a redundant or complementary role, in cardiac muscle, performing the basic functions of nebulin in skeletal muscle. Alternatively, our investigations will likely discover potential novel functions for nebulette in cardiac muscle. Our future studies will address these possibilities in detail.

REFERENCES

Bang, M.L., Gregorio, C., and Labeit, S. (2002). Molecular dissection of the interaction of desmin with the C-terminal region of nebulin. J Struct Biol *137*, 119-127.

Bar, H., Fischer, D., Goudeau, B., Kley, R.A., Clemen, C.S., Vicart, P., Herrmann, H., Vorgerd, M., and Schroder, R. (2005a). Pathogenic effects of a novel heterozygous R350P desmin mutation on the assembly of desmin intermediate filaments in vivo and in vitro. Hum Mol Genet *14*, 1251-1260.

Bar, H., Mucke, N., Kostareva, A., Sjoberg, G., Aebi, U., and Herrmann, H. (2005b). Severe muscle disease-causing desmin mutations interfere with in vitro filament assembly at distinct stages. Proc Natl Acad Sci USA *102*, 15099-15104.

Bar, H., Schopferer, M., Sharma, S., Hochstein, B., Mucke, N., Herrmann, H., and Willenbacher, N. (2010). Mutations in desmin's carboxy-terminal "tail" domain severely modify filament and network mechanics. J Mol Biol *397*(5), 1188-1198.

Conover, G.M., Henderson, S.N., and Gregorio, C.C. (2009). A myopathy-linked desmin mutation perturbs striated muscle actin filament architecture. Mol Biol Cell *20*, 834-845.

Goebel, H.H. (1995). Desmin-related neuromuscular disorders. Muscle Nerve *18*, 1306-1320.

Goldfarb, L.G., and Dalakas, M.C. (2009). Tragedy in a heartbeat: malfunctioning desmin causes skeletal and cardiac muscle disease. J Clin Invest *119*, 1806-1813.

Herrmann, H., Bar, H., Kreplak, L., Strelkov, S.V., and Aebi, U. (2007). Intermediate filaments: from cell architecture to nanomechanics. Nat Rev Mol Cell Biol *8*, 562-573.

Herrmann, H., Strelkov, S.V., Burkhard, P., and Aebi, U. (2009). Intermediate filaments: primary determinants of cell architecture and plasticity. J Clin Invest *119*, 1772-1783.

Holmes, W.B., and Moncman, C.L. (2008). Nebulette interacts with filamin C. Cell Motil Cytoskeleton *65*, 130-142.

Kazmierski, S.T., Antin, P.B., Witt, C.C., Huebner, N., McElhinny, A.S., Labeit, S., and Gregorio, C.C. (2003). The complete mouse nebulin gene sequence and the identification of cardiac nebulin. J Mol Biol *328*, 835-846.

Kruger, M., Wright, J., and Wang, K. (1991). Nebulin as a length regulator of thin filaments of vertebrate skeletal muscles: correlation of thin filament length, nebulin size, and epitope profile. J Cell Biol *115*, 97-107.

Lazarides, E., and Hubbard, B.D. (1976). Immunological characterization of the subunit of the 100 A filaments from muscle cells. Proc Natl Acad Sci USA *73*, 4344-4348.

Littlefield, R.S., and Fowler, V.M. (2008). Thin filament length regulation in striated muscle sarcomeres: pointed-end dynamics go beyond a nebulin ruler. Semin Cell Dev Biol *19*, 511-519.

McElhinny, A.S., Kolmerer, B., Fowler, V.M., Labeit, S., and Gregorio, C.C. (2001). The N-terminal end of nebulin interacts with tropomodulin at the pointed ends of the thin filaments. J Biol Chem *276*, 583-592.

Moncman, C.L., and Wang, K. (1995). Nebulette: a 107 kD nebulin-like protein in cardiac muscle. Cell Motil Cytoskeleton *32*, 205-225.

Moncman, C.L., and Wang, K. (2000). Architecture of the thin filament-Z-line junction: lessons from nebulette and nebulin homologies. J Muscle Res Cell Motil *21*, 153-169.

Omary, M.B. (2009). "IF-pathies": a broad spectrum of intermediate filament-associated diseases. J Clin Invest *119*, 1756-1762.

Ottenheijm, C.A.C., Witt, C.C., Stienen, G.J., Labeit, S., Beggs, A.H., and Granzier, H. (2009). Thin filament length dysregulation contributes to muscle weakness in nemaline myopathy patients with nebulin deficiency. Hum Mol Genet *18*, 2359-2369.

Panaviene, Z., Deng, X.A., Esham, M., and Moncman, C.L. (2007). Targeting of nebulin fragments to the cardiac sarcomere. Exp Cell Res *313*, 896-909.

Panaviene, Z., and Moncman, C.L. (2007). Linker region of nebulin family members plays an important role in targeting these molecules to cellular structures. Cell Tissue Res *327*, 353-369.

Pelin, K., Donner, K., Holmberg, M., Jungbluth, H., Muntoni, F., and Wallgren-Pettersson, C. (2002). Nebulin mutations in autosomal recessive nemaline myopathy: an update. Neuromuscul Disord *12*, 680-686.

Pelin, K., Hilpela, P., Donner, K., Sewry, C., Akkari, P.A., Wilton, S.D., Wattanasirichaigoon, D., Bang, M.L., Centner, T., Hanefeld, F., Odent, S., Fardeau, M., Urtizberea, J.A., Muntoni, F., Dubowitz, V., Beggs, A.H., Laing, N.G., Labeit, S., de la Chapelle, A., and Wallgren-Pettersson, C. (1999). Mutations in the nebulin gene associated with autosomal recessive nemaline myopathy. Proc Natl Acad Sci USA *96*, 2305-2310.

Sanoudou, D., and Beggs, A.H. (2001). Clinical and genetic heterogeneity in nemaline myopathy--a disease of skeletal muscle thin filaments. Trends Mol Med *7*, 362-368.

Tonino, P., Pappas, C.T., Hudson, B.D., Labeit, S., Gregorio, C.C., and Granzier, H. (2010). Reduced myofibrillar connectivity and increased Z-disk width in nebulin-deficient skeletal muscle. J Cell Sci *123*, 384-391.

Wang, K. (1981). Nebulin, a giant protein component of N2 line striated muscle. J. Cell Biology *91*, 335a.

Youssef, N.C., Scola, R.H., Lorenzoni, P.J., and Werneck, L.C. (2009). Nemaline myopathy: clinical, histochemical and immunohistochemical features. Arq Neuropsiquiatre *67*, 886-891.

CONTACT INFORMATION

Name:	Krystyna Marie Jacobs
Professional Address:	c/o Dr. Gloria Conover Department of Veterinary Pathobiology MS 4467 Texas A&M University College Station, TX 77843
Email Address:	krystynamj@gmail.com
Education:	B.S., Biomedical Science, Texas A&M University, August 2010 Undergraduate Research Scholar